Triplet Radical Interaction. Direct Measurement of Triplet Polarization Transfer by Fourier Transform Electron Paramagnetic Resonance

Aharon Blank and Haim Levanon*

Department of Physical Chemistry and the Farkas Center for Light-Induced Processes, The Hebrew University of Jerusalem, 91904 Israel

Received: July 14, 1999; In Final Form: October 19, 1999

An FT-EPR (Fourier transform electron paramagnetic resonance) method for the direct measurement of the electron spin polarization generated in stable radicals through photoexcited triplet and radical interaction is presented. This method depends on the ability to calculate numerically the filling factor of the irradiated volume in the EPR cavity. By this experimental method the polarization at different times after the laser pulse can be determined. This enables us to differentiate between the different processes generating the polarization in the radical, which are the ESPT (electron spin polarization transfer), when the triplet meeting the radical is still polarized, and the RTPM (radical triplet pair mechanism), for thermal triplets. The different time evolutions of the two mechanisms allow the spin−lattice relaxation time (T_1) of the triplet in liquid solution to be determined. Experimental verifications were made with galvinoxyl-porphyrin systems in toluene at different temperatures.

I. Introduction

Since its discovery,[1] two main mechanisms have been associated with chemically induced dynamic electron polarization (CIDEP), namely, the triplet mechanism (TM)[2] and the radical pair mechanism (RPM).[3] In the former, the electron spin polarization (ESP) is generated by selective intersystem crossing (ISC) from the photoexcited singlet to the triplet state, and in the latter, ESP is generated through collisions between radicals. Following the widespread use of lasers in EPR experiments, there have been some new observations of CIDEP of stable radicals in solution in the presence of photoexcited triplet chromophores. This polarization could not be explained by the above mechanisms and was treated theoretically[4−7] and experimentally[8−13] by means of the radical triplet pair mechanism (RTPM).

The theory of RTPM is mainly associated with the radical's polarization, which is generated during the interaction of radicals with the photoexcited triplets. Current theories provide analytical[5−8] and numerical[10] results for the dependence of the spin polarization upon the zero-field splitting (ZFS) parameter (D), solvent viscosity (ρ), and triplet radical electron spin exchange (J). According to RTPM theory, the observed net polarization, which is equal for all hyperfine lines, depends on the precursor state (photoexcited singlet or triplet) and the sign of J.[14,15] Thus, for $J < 0$ the sign of polarization is negative for a triplet precursor and positive for a singlet one. The opposite holds for $J > 0$.[16] In addition to the net polarization, a multiplet polarization also exists, resulting in different polarization for the different hyperfine lines, which is usually much smaller in magnitude. A deeper understanding of RTPM requires additional experimental approaches to reveal accurately the polarization dependence in wide spectrum of systems under various conditions.

The majority of experimental techniques dealing with this problem have been associated with continuous-wave time-resolved EPR (CW-TREPR) spectroscopy to monitor the radical spectrum after generation of the triplet by the laser pulse. By careful analysis of the EPR kinetics, combined with independent knowledge of the rate constants involved, one can acquire a good estimate of the radical polarization. However, this method suffers from some difficulties, which prevent extensive and accurate measurements of the radical polarization in various systems under different external conditions (i.e., temperature). Moreover, when the triplet is polarized, during its spin−lattice relaxation time (T_1^T), the polarization of the radical is completely different from that generated when an unpolarized triplet interacts with the radical,[11] which further complicates the polarization measurements.

In this study we demonstrate that these difficulties can be circumvented by employing a special pulsed laser-microwave phase-cycling (PLMPC). We will show the feasibility of these experiments through some examples for polarization acquisition at different temperatures. The investigated systems are galvinoxyl free radical (Gal), 2,6-di-*tert*-butyl-α-(3,5-di-*tert*-butyl-4-oxo-2,5-cyclohexadien-1-ylidene)-*p*-tolyloxy in the presence of free base tetraphenylporphyrin and zinc−tetraphenylporphyrin (H_2TPP and ZnTPP, respectively) all dissolved in toluene. In addition to RTPM polarization, these systems exhibit an electron spin polarization transfer mechanism (ESPT), which accounts for the emissive spectrum of the radical with H_2TPP and the enhanced absorptive one for that with ZnTPP.[11] Within the time interval that the porphyrin triplet is polarized, the ESPT mechanism is dominant, while later in time, the RTPM takes over. Both mechanisms result in polarized radicals with different characteristics.

The relevant photophysical reactions involved are

$$P \xrightarrow{h\nu} {}^1{*}P \xrightarrow{ISC} {}^3{*}P_p \tag{1}$$

$${}^3{*}P_p + R \xrightarrow{ESPT} R_p \tag{2}$$

$${}^3{*}P + R \xrightarrow{RTPM} R_p \tag{3}$$

10.1021/jp992379l CCC: $19.00
Published on Web 01/06/2000

where P and R are the porphyrin and radical molecules, respectively, and the subscript p stands for polarized state.

The capability of our experimental approach to differentiate between the two mechanisms is demonstrated in these systems. This quantification also enables us to directly gain a good estimate of the triplet spin−lattice relaxation time in liquid solution, where its EPR signal cannot be detected. On the basis of existing RTPM theories and the polarization measurements, we will estimate the magnitude of the triplet radical exchange interaction constant and its distance dependence. Finally, we comment on the difference between the experimental methods of CW-TREPR[8,11] and the pulsed method presented here.

II. Experimental Section

H_2TPP, Gal, toluene (Aldrich), and ZnTPP (Midcentury Chemical Co.) were used without further purification. Samples were prepared by dissolving in a Pyrex tube (inner and outer diameters of 2.8 and 4 mm, respectively) the stable Gal and the porphyrin in toluene and then sealing under vacuum after several freeze−thaw cycles. FT-EPR measurements were performed with a Bruker ESP 380E spectrometer. Linear prediction was used for the dead-time free induction decay (FID) reconstruction.[17] The porphyrins in the mixture were photoexcited by a Continuum laser model 661-2D ($\lambda = 532$, pulse duration 12 ns, pulse repetition rate 20 Hz, and pulse energy 5 mJ per pulse). The triplet concentrations in the irradiated volume were estimated to be ∼0.1 and ∼0.5 mM for H_2TPP and ZnTPP, respectively, taking into account the laser energy and porphyrin extinction coefficient for a concentration of ∼1 mM.[18] Radical concentrations were ∼0.1 and ∼0.15 mM for the Gal-H_2TPP and Gal-ZnTPP samples, respectively.

Some of the experiments in this research required the evaluation of the difference between the signals with and without laser excitation. Direct subtraction of the results of the two modes was not reliable due to the very small differences in the EPR signals between the two experiments (with and without the laser). Therefore, we have employed an alternate method, i.e., PLMPC, which is more sensitive and can detect very small differences. In this experimental mode, each laser pulse triggers the desired pulse sequence, followed by an identical pulse sequence (25 ms later in time) but without the laser excitation. In the second sequence, the signal amplitude is inverted, i.e., multiplied by −1, by using an inverting video amplifier with unit amplification. The signals from these two processes are averaged on the digitizer (Lecroy model 9400). This PLMPC enables us to obtain directly the difference between the EPR signals (with and without photoexcitation) in a single experiment. Thus, with sufficient averaging, even small signal differences can be measured and analyzed. The detailed description of the PLMPC pulse sequence will be discussed in the next section.

III. Results and Discussion

a. Pulse Sequence. Before discussing the pulse sequence and its effect on the polarization pattern, we will discuss some of the difficulties in employing CW-TREPR in these type of experiments. On the basis of the expressions of Verma and Fessenden[19] and Blättler et al.,[4] let us examine typical kinetic equations for the RTPM process observed by CW-TREPR. Upon resonance of a particular EPR line, the following modified Bloch equations govern the RTPM process and describe the magnetization of the radical:

$$\frac{dM_y}{dt} = -\frac{M_y}{T_2^R} - \omega_1 M_z - k_q M_y[T] \quad (4)$$

$$\frac{dM_z}{dt} = \omega_1 M_y + \frac{P_{eq}[R]' - M_z}{T_1^R} + k_q(P_n \pm P_m)[T][R]' \quad (5)$$

$$\frac{d[T]}{dt} = -k_q[T][R] - 2k_{TT}[T]^2 - k_T[T] \quad (6)$$

where P_{eq} is the equilibrium Boltzmann polarization, P_n and P_m are the net and multiplet polarizations, respectively, ω_1 is proportional to the microwave power, and k_q is the triplet radical quenching rate constant. [T] is the triplet concentration and $[R]' = [R]\mu_B$, where [R] is the radical concentration and μ_B is the Bohr magneton. k_{TT} is the triplet−triplet quenching rate constant and k_T is the triplet decay rate; M_y, M_z, T_1^R, and T_2^R are the conventional magnetic resonance variables of the radical.[20] In CW-TREPR experiments, we measure time evolution of M_y with a typical time constant of 100 ns. Therefore, a parametric line fit to P_n, P_m, and T_1^R from the experimental kinetic curve requires a time frame of at least $3T_1^R$ observation time for meaningful and accurate results. It implies that within this time frame, one cannot neglect changes in triplet concentration and eqs 4−6 become coupled. Thus, all the relevant rate constants must be taken into account in the kinetics line fit. Results of such a multiparameter fit cannot be adequate, unless the different rate constants at various conditions are known independently. Furthermore, as stated above, recent studies show[11] that radical polarization may result from a combination of two spin polarization mechanisms, i.e., RTPM and ESPT. The latter mechanism occurs if the photoexcited triplet is created in a polarized state and can transfer its polarization to the radical, as long as it exists (∼$3T_1^R$ of the triplet). This ESPT mechanism complicates the problem of sorting out the different polarization mechanisms acquired by the radical, making the problem difficult to be solved quantitatively by CW-TREPR. Accurate knowledge of the polarization is important for determining the actual mechanism that occurs during triplet radical encounters and also to assess the exchange interaction, and its distance dependence.

The difficulties associated with CW-TREPR measurements can be overcome by utilizing a simple pulsed EPR technique from which the ESPT and RTPM polarizations can be obtained directly. Two PLMPC modes were employed. The first sequence consists of $\pi/2-\tau-$laser pulse$-\tau_1-\pi-$echo detection (Figure 1a). We can analyze this sequence by a simple vector model for the magnetization. The first pulse rotates the magnetization into the laboratory *XY* plane, and without the laser pulse, the sequence is a simple Hahn echo experiment. On the other hand, the laser pulse generates the triplets in solution (usually within a time scale of a few nanoseconds), which encounter with the stable radicals. Each encounter results in phase loss of the magnetization in the *XY* plane and a generation of polarization in the *Z* axis (cf. eqs 4−5). Thus, these encounters reduce the echo amplitude relative to the sequence with the laser pulse absent. The second pulse experiment measures the magnetization in the *Z* axis by the sequence, $\pi/2-\tau-$laser pulse$-(2\tau_1 + \tau)-\pi/2-$FID detection (Figure 1b). This sequence is similar to the previous one, except that at the time of the echo appearance in the first sequence, the *Z*-axis magnetization is now measured by FID.

We now examine quantitatively the radical kinetics associated with these two sequences. Starting with the first sequence, we differentiate between two regions of the sample. One region,

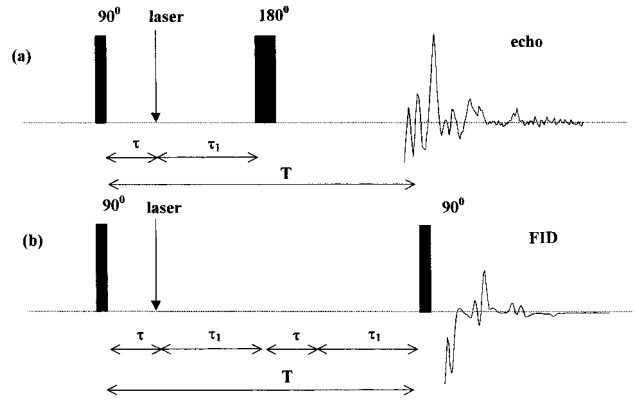

Figure 1. (a) Echo pulse sequence to determine the rate of triplet radical encounters. (b) FID pulse sequence to determine the Z magnetization induced by the polarization processes. The duration of all of the pulses is negligible. A typical echo and FID are also provided.

with a filling factor of η_1, is not exposed to photoexcitation but contributes to the EPR signal of the radical. The second region, with a filling factor of η_2, is exposed to the photoexcitation. We also define $\eta_T = \eta_1 + \eta_2$, where η_T is the filling factor of the entire sample volume. It is noteworthy that the term "filling factor" in the CW case[21,22] is somewhat different from that in the pulsed microwave case. For that purpose, we have derived the expressions for calculating the filling factor for the pulsed case.[23] The differentiation between the exposed and unexposed regions to light is made with the reasonable assumption that the diffusion of the species is much less than ~1 cm/s;[24] thus, it is assumed that within the time scale of the experiment (<10 μs) the two regions do not mix.

Evidently, the magnetization in region 1 will be independent of the laser excitation, implying that after the first $\pi/2$ microwave (mw) pulse, the time dependence of M_{1y} from this region is described by

$$\frac{dM_{1y}}{dt} = -\frac{M_{1y}}{T_2^R} \tag{7}$$

The magnetization in region 2 should obey a different rate expression (cf. eq 4, with no microwave power):

$$\frac{dM_{2y}}{dt} = -\frac{M_{2y}}{T_2^R} - k_q[T]M_{2y} \tag{8}$$

We assume that the photoexcited triplet and radical concentrations are not larger than ~1 mM and we will observe the signal evolution in a time window of ~100 ns, well above the time resolution of the FT-EPR experiment. Therefore, taking into account the diffusion rates in toluene, the changes in [T] can be neglected. With this assumption, eqs 7 and 8 can be solved analytically, i.e.

$$M_{1y}(t) = M_{1y}^0 e^{-t/T_2^R} \tag{9}$$

$$M_{2y}(t) = M_{2y}^0 e^{-t(1/T_2^R + k_q[T])} \tag{10}$$

To obtain a quantity proportional to the EPR signal from a specific region, we must multiply the magnetizations M_{1y} and M_{2y} by the corresponding filling factors. Thus, without laser excitation (OFF), the voltage, V^{OFF}, of the EPR signal is given by

$$V^{OFF}(t) = \eta_T M_y^0 e^{-t/T_2^R} \tag{11}$$

We have used the fact that after the first $\pi/2$ mw pulse, $M_{1y}^0 = M_{2y}^0 \equiv M_y^0$. Upon laser excitation (ON), the EPR signal is given by

$$V^{ON}(t) = (\eta_T - \eta_2)M_y^0 e^{-t/T_2} + \eta_2 M_y^0 e^{-t(1/T_2 + k_q[T])} \tag{12}$$

Therefore, the difference between the signal magnitudes becomes

$$V^{ON}(t) - V^{OFF}(t) = M_y^0 \eta_2 [e^{-t(1/T_2^R + k_q[T])} - e^{-t/T_2^R}] \tag{13}$$

Now, let us consider the second pulse sequence and the FID detection. Using the same notation and assumptions as above and differentiating between the two regions (exposed and unexposed to laser excitation), we obtain from the Bloch equations (cf. eq 5, with no microwave power)

$$\frac{dM_{1z}}{dt} = \left(\frac{P_{eq}[R]' - M_{1z}}{T_1^R}\right) \tag{14}$$

$$\frac{dM_{2z}}{dt} = \left(\frac{P_{eq}[R]' - M_{2z}}{T_1^R}\right) + k_q(P_n \pm P_m)[T][R]' \tag{15}$$

From which we can obtain the analytical solutions for the two regions:

$$M_{1z}(t) = P_{eq}[R]' + (M_{1z}^0 - P_{eq}[R]')e^{-t/T_1^R} \tag{16}$$

$$M_{2z}(t) = P_{eq}[R]' + k_q T_1^R (P_n \pm P_m)[T][R]' + (M_{2z}^0 - P_{eq}[R]' - k_q T_1^R (P_n \pm P_m)[T][R]')e^{-t/T_1^R} \tag{17}$$

Thus, for the second pulse sequence, the difference between the induced EPR signals with the laser ON and OFF is

$$V^{ON}(t) - V^{OFF}(t) = \eta_2 k_q[T]T_1(P_n \pm P_m)[R]'(1 - e^{-t/T_1^R}) + (M_{2z}^0 - M_{1z}^0)e^{-t/T_1^R}\eta_2 \tag{18}$$

Two cases should be considered: (a) The simple one is where the polarization generated at each encounter is time independent; i.e., only RTPM is operative (in this case T_1^T of the triplet is very short and thus the ESPT is negligible). In such a case, the initial conditions can be chosen such that $(M_{2z}^0 - M_{1z}^0)$ in eq 18 is negligibly small (this is obtained because after the first $\pi/2$ mw pulse the Z magnetization is negligibly small). For this case, eq 18 describes the signal difference as long as the triplet concentration does not change significantly (a few microseconds in our experiments). (b) In the general case, both ESPT and RTPM are operative. Therefore, the polarization generated in each triplet radical encounter can change significantly with a time constant typical of the triplet spin−lattice relaxation (order of ~0.1 μs for our case). In this case, the application of eq 18 is carried out along different time windows with different polarization values used for each window (it is assumed that within these short intervals of several ~10 ns, the polarization is constant, namely $T_1^T \gg 10$ ns).

In this paragraph we describe how to manipulate eqs 13 and 18 in order to obtain the radical polarization at different times. Equation 13 reflects the difference between the spin echo amplitude as a function of τ_1 (Figure 1a) with and without the laser excitation. For the initial condition of eq 13 we obtain the value of $M_y^0\eta_2$ by first measuring the value of $M_y^0\eta_T$ and then multiplying it by η_2/η_T to obtain the value of $M_y^0\eta_2$. The value $M_y^0\eta_T$ is measured by the first pulse sequence, without laser

irradiation with the π mw pulse given at $\tau/2$ ($\tau_1 = -\tau/2$) and the echo appears at τ (Figure 1a). The relation η_2/η_T can be found numerically through a recently developed method.[22] The pulse sequence shown in Figure 1a employs the laser pulse after the $\pi/2$ mw pulse. This is required by eq 13 to obtain the initial condition M_y^0, which is independent upon laser excitation. The value of T_2 without the laser pulse can be measured by any conventional FT-EPR method. This leaves us with a single unknown parameter, $A \equiv k_q[T]$. This parameter can be obtained by recording the echo amplitude in short intervals of τ_1 (with a time window of ~100 ns) and employing a curve fitting of eq 13. Once A is known, the only unknown parameter is $P_n \pm P_m$ in eq 18. The radical magnetization at equilibrium, which is related to $\eta_2[R]'$ in eq 18, is obtained by the FID following the $\pi/2$ mw pulse. The FID amplitude is simply $\eta_T[R]'P_{eq}$, which, when multiplied by $\eta_L/(\eta_T P_{eq})$,[22,23] yields $\eta_L[R]'$. It should be noted that T_1^R is found independently by conventional pulsed EPR techniques. Therefore, we can conclude that the above procedure enables us to obtain first $k_q[T]$, which is a single curve-fitting parameter (eq 13), with which we can obtain directly and accurately $P_n \pm P_m$, again as a single curve-fitting parameter (eq 18). It is noteworthy that in contrast to CW-TREPR, the accurate knowledge of the radical and triplet concentration and the various diffusion rate constants involved is not required.

An important experimental issue is related to the actual measurement of $V^{ON}(t) - V^{OFF}(t)$ in eq 13. In our case, the difference $V^{ON}(t) - V^{OFF}(t)$ is on the order of $V^{OFF}/100$. This is due to the fact that the laser illuminates only part of the sample and the diffusion-controlled process of encounters requires some time to develop (~100 ns). Thus, performing two experiments (with and without laser) and then subtracting the signals is not practical and the difference will be lost in the noise. The experimental method introduced here (cf. Experimental) circumvents the difficulties in evaluating the signal difference, $V^{ON}(t) - V^{OFF}(t)$.

The derivation presented in this chapter can be made independently for each hyperfine line of the radical and, thus, one can extract, for any specific line, its T_2^R, and polarization.

b. Triplet Radical Encounters. With the above experimental procedure, we have measured the triplet quenching rate and the electron spin polarization generated in mixtures of Gal-H_2TPP and Gal-ZnTPP dissolved in toluene at different temperatures. In our measurements, within experimental accuracy, the entire hyperfine lines exhibit similar T_2^R, and the multiplet polarization was found to be small compared to the net polarization. Therefore, the results refer to all the radical hyperfine lines.

i. Triplet Quenching Rate. Figure 2 shows the FT-EPR spectra of the Gal radical and the spectrum of Gal-H_2TPP and Gal-ZnTPP following the laser pulse. The observed triplet radical spectra consist of three contributions, i.e., from polarized radicals due to the interaction between stable radicals and photoexcited triplets, from stable radicals outside the illuminated region, and from nonreactive radicals in the illuminated region. It can be seen that in the case of Gal-H_2TPP, the spectrum is in emission, implying that the polarized magnetization from the illuminated region dominates the spectrum. In the Gal-ZnTPP system, the thermal spectrum (in absorption) is enhanced due the fact that the illuminated region contributes polarized radicals in enhanced absorption.

Figure 3 presents the difference in signal intensities obtained for the echo pulse sequence ($V^{ON} - V^{OFF}$) for the two porphyrins systems in toluene, at 230 K. For H_2TPP, the diffusion-controlled rate of triplet−triplet quenching can be estimated via

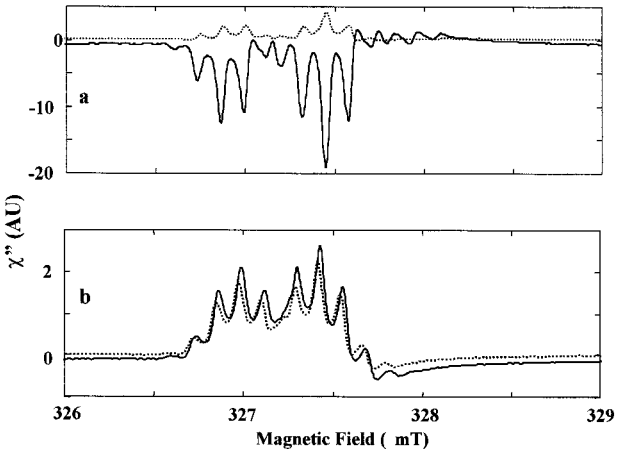

Figure 2. (a) Polarized FT-EPR spectrum (in emission) of the Gal radical after laser irradiation in a solution with H_2TPP (solid line). The dashed line is the spectrum with the laser OFF. (b) The same as (a), but for Gal-Zn. The deviation from binomial intensities is due to the limited bandwidth of the spectrometer, as the spectrum was taken at a single fixed point in the middle. The differences in the intensities between the two species reflect the polarization difference.

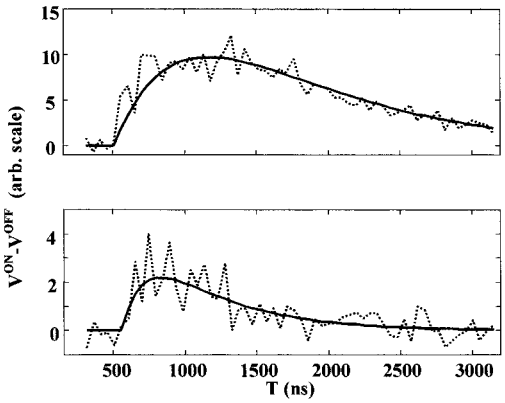

Figure 3. (a) $V^{ON} - V^{OFF}$ for the echo pulse sequence for Gal-H_2TPP in toluene at 230 K. (b) The same as (a) but for Gal-ZnTPP. The solid line is the theoretical results obtained via eq 13 with a single parameter fit ($A = k_q[T]$). $M_y^0\eta_L$ and T_2^R are measured independently (see text). The abscissa represents the time after the first $\pi/2$ mw pulse (Figure 1). The laser pulse was triggered ~580 ns after the first $\pi/2$ mw pulse. The data plotted here and in Figures 4−6 were taken on the strongest hyperfine line, which represents well the entire hyperfine lines, after FFT of the echo or FID. This is because T_2^R was found to be similar in all the lines and the multiplet polarization was negligible.

eq 19,[25] where R is the gas constant, T is the temperature, and

$$k_d = 8RT/3\rho \qquad (19)$$

ρ is the viscosity. For $\rho = 1.13$ cP,[8] k_d was found to be 4.5×10^9 M^{-1} s^{-1}. With the estimated triplet concentration of ~0.1 mM for the H_2TPP (see above), it is evident that for the first microsecond, the initial triplet concentration is affected only by 10%−20%. The small change in the triplet concentration is in line with our assumptions, which were used to derive the kinetic eqs 13 and 18. However, for the ZnTPP system, the higher concentration of the triplet (about 0.5 mM) leads to an apparent change in the triplet concentration with the first microsecond after the laser pulses (cf. Figure 3b). From the echo experiments, with no laser excitation, we could extract the radical relaxation time (T_2^R) for our two samples, which was found to be 760 ± 30 and 530 ± 25 ns for Gal-H_2TPP and Gal-ZnTPP, respectively. The experimental data of Figure 3 were treated via eq 13 with a single variable parameter, $k_q[T]$,

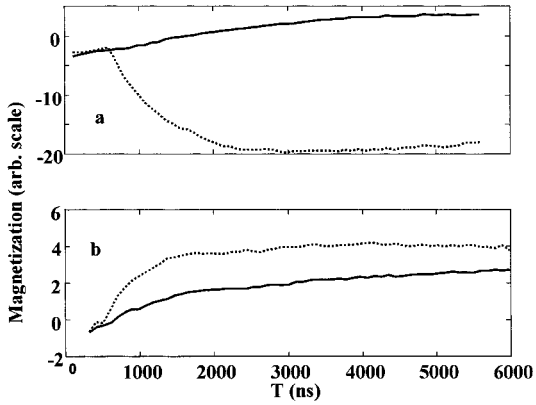

Figure 4. (a) FID pulse sequence signal for Gal-H_2TPP in toluene at 230 K (solid line, laser OFF; dashed line, laser ON). (b) The same as (a) but for Gal-ZnTPP. The abscissa represents the time after the first $\pi/2$ mw pulse (see Figure 1).

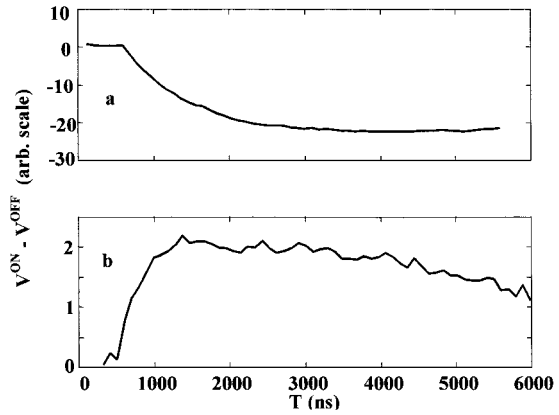

Figure 5. (a) $V^{ON} - V^{OF}$ in the FID pulse sequence for Gal-H_2TPP and (b) for Gal-ZnTPP in toluene at 230 K. The abscissa represents the time after the first $\pi/2$ mw pulse (see Figure 1).

found to be $(4.4 \pm 0.3) \times 10^5$ and $(2.5 \pm 0.2) \times 10^6$ s^{-1} for Gal-H_2TPP and the Gal-ZnTPP, respectively. These values are in line with our independent estimation of triplet concentration and the diffusion-controlled rate constant (eq 19). The ratio η_2/η_T for the FID experiments was calculated to be 0.5 and 0.1 for Gal-H_2TPP and Gal-ZnTPP, respectively,[22,23] and 0.52 and 0.11 for the echo experiments, respectively.[22,23] The different η_2/η_T in the two samples is due to the different experimental conditions, e.g., η_2 vs η_1.[18]

ii. Polarization Measurements. We show in Figure 4 the measured FID amplitude of the Gal signal following the two $\pi/2$ mw pulse sequences (Figure 1b), with and without laser irradiation. When the laser is OFF, the signal amplitude slowly approaches thermal equilibrium within 2900 ± 200 and 2000 ± 150 ns for Gal-H_2TPP and Gal-ZnTPP, respectively. These values should be attributed to the spin−lattice relaxation time T_1^R of the Gal radical. Upon photoexcitation, about 580 ns after the first $\pi/2$ mw pulse, the magnetization is created much faster than T_1^R. This is due to the radicals undergoing encounters with the photoexcited porphyrins, causing their magnetization to be transferred nonadiabatically into the laboratory Z axis (M_z), with a non-Boltzmann polarization.

Figure 5 presents the amplitude difference ($V^{ON} - V^{OFF}$) described in eq 18, in the two $\pi/2$ mw pulse experiments. This is carried out by subtracting the two corresponding lines in Figure 4. Let us examine the results of the Gal-H_2TPP system (Figure 5a). First, it is noticed that the generated polarization is negative, i.e., in emission. Inspection of eq 18 shows that for

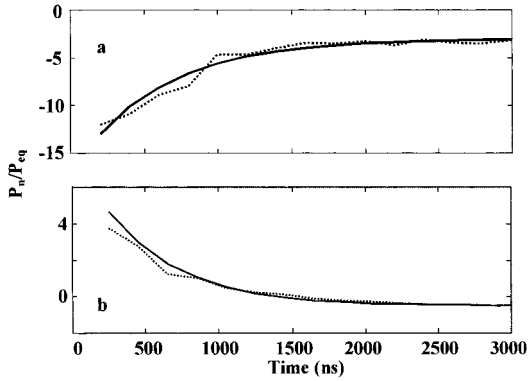

Figure 6. (a) Polarization curve of Gal-H_2TPP polarization as a function of time after laser pulse (dotted curve) fitted by eq 20 (solid line). All the fitting parameters are given in Table 1. The abscissa represents the time after the laser pulse (see Figure 1).

constant polarization (P_n), the signal should approach asymptotically to a constant value with the characteristic time of T_1^R, i.e., ~ 2.9 μs. However, the experimental results shows that ($V^{ON} - V^{OFF}$) approaches a constant value at ~ 1.5 μs, which corresponds to an apparently much smaller characteristic time. To explain this discrepancy, the two polarization mechanisms ESPT and RTPM should be considered.[11] The ESPT, which is the polarization transfer from the polarized triplet porphyrin is dominant in early times after laser excitation. This mechanism is operative during the spin−lattice relaxation time of the triplet state (T_1^T). The RTPM contributes a much smaller polarization (in our case) but within a much longer time window, i.e., the triplet lifetime. Thus, P_n in eq 18 is time dependent because it is essentially the average apparent polarization, which results from the combination of these two mechanisms. Equation 18 is the general description of the polarization created by either ESPT or RTPM processes. Thus, a best-fit analysis was carried out for different short times (200−300 ns) along the experimental curve in Figure 5 to obtain the polarization values valid for this time window (assuming it does not change significantly during this time, as discussed in the previous section). Except for the polarization, all the values in eq 18 are known and, consequently, the curve fit is reliable and requires very few points of ($V^{ON} - V^{OFF}$) vs time. This fitting procedure provides the polarization as a function of time (Figure 6).

Considering the two polarization mechanisms, quantitative description of the net polarization vs time is given by

$$P_n(t) = P_n^{ESPT} e^{-t/T_1^T} + (1 - e^{-t/T_1^T}) P_n^{RTPM} \qquad (20)$$

where P_n^{ESPT} and P_n^{RTPM} are the polarization created in the ESPT and RTPM processes, respectively, and the T_1^T values are of the photoexcited triplet. Curve fitting of the experimental lines for Gal-H_2TPP and Gal-ZnTPP (Figure 6) was carried out with eq 20, and the results are presented in Table 1. Additional results were obtained for both systems at 210 and 250 K (Table 1).

We now discuss and compare the experimental polarization results with those obtained theoretically. First, let us consider the ESPT case. With the analysis carried out previously for different systems,[26−28] one would expect the triplet polarization of H_2TPP to be about $-15P_{eq}$, at 230 K. This value is very close to the results obtained here for the ESPT polarization. The polarization of ZnTPP should be, according to the same treatment,[28] about $55P_{eq}$, which is much larger than the value we obtained for ESPT polarization. Although a full theoretical treatment for the ESPT mechanism is not yet available, we

TABLE 1: Polarization Parameters of Gal-H_2TPP and Gal-ZnTPP

T (K)	T_1 (ns)	P^{ESPT} (exp)	P^{RTPM} (exp)	D_r (10^{-5} cm^2 s^{-1})	P^{RTPM} (calc)[a]	ρ (cP)[b]
			a. Gal-H_2TPP			
210	700 ± 35	-18 ± 1	-5 ± 0.5	0.45	-5.15	1.54
230	600 ± 30	-17 ± 1	-3 ± 0.3	0.67	-3.4	1.13
250	500 ± 25	-16 ± 1	-2.5 ± 0.25	0.95	-2.4	0.87
			b. Gal-ZnTPP			
210	700 ± 35	7 ± 1	-1.7 ± 0.17	0.45	-1.6	1.54
230	400 ± 20	8 ± 1	-0.5 ± 0.05	0.67	-1	1.13
250	300 ± 15	9 ± 1	-0.3 ± 0.03	0.95	-0.7	0.87

[a] Calculated results for RTPM with strong exchange limit. [b] Solvent viscosity.

believe that the exchange interaction between the radical and the triplet is of importance, as suggested recently.[11] In order for the ESPT process to be efficient, the exchange interaction in terms of $J(r) = J_0 \exp[-\lambda(r - d)]$[29] must be much larger than the inverse of the encounter time at the closest approach distance (d), where the exchange interaction is dominant. Using the equation $\tau_\Delta = d^2/D_r$,[29] we can estimate the encounter time for our systems at 230 K to be $\tau_\Delta = 1.2 \times 10^{-9}$ s. J_0 and λ were estimated using the RTPM results and are detailed bellow. The free parameter λ is found to be much larger for ZnTPP than for H_2TPP, i.e., 4 and 2 Å^{-1}, respectively. Moreover, J_0 is found to be smaller for Gal-ZnTPP than for Gal-H_2TPP (-1.2×10^{10} and -2.5×10^{10} s^{-1}, respectively). Thus, for Gal-ZnTPP, $J(r)$ decreases rapidly and consequently the ESPT at the encounter distance is inefficient.

We now discuss the calculated RTPM polarization results given in Table 1. When examining the polarization results for Gal-H_2TPP, one must consider the relationship between the exchange interaction (J_0) and the Zeeman splitting ($g\beta B$), i.e., $g\beta B < J_0 > g\beta B$. We have examined the case of the weak exchange interaction by the method described previously,[6,30] with the diffusion coefficient of the relevant species, shown in Table 1. The diffusion coefficients were obtained with the Stokes−Einstein equation:

$$D_r = k_B T/6\pi\rho a \qquad (21)$$

The values for the effective hydrodynamic radii (a) of H_2TPP (or ZnTPP) were taken as 5 Å[7] and for Gal the radius was estimated to be 4 Å. The attempt to explain the results under the assumption of weak exchange interaction limit was unsatisfactory and could not account for the experimental polarization values (Table 1).[30] Thus, the strong limit of the exchange interaction should be considered. In this case, we can calculate the polarization for Gal-H_2TPP with the analytical expression given elsewhere,[6,30,31] and the results are summarized in Table 1. The parameters used for the calculation of the polarization are the ZFS parameter $D = 318$ G, X-band mw frequency, a rotational correlation time of 200 ps, and the adjustable parameters $J_0 = -16 \times 10^{10}$ rad/s and $\lambda = 2$ Å^{-1}. On the other hand, attempts to calculate the polarization in Gal-ZnTPP (Table 1) were less successful. The calculation employed the same parameters as for Gal-H_2TPP, but with $J_0 = -8 \times 10^{10}$ rad/s and $\lambda = 4$ Å^{-1}. As already discussed above for the ESPT case, the exchange interaction is weaker in ZnTPP and decreases more rapidly with distance; thus it does not fully correspond to the strong exchange approximation. This may be the reason for the discrepancies that still exist in this case between the calculated and experimental results. A possible explanation for the different exchange interaction parameters for the two similar porphyrins can be attributed to the fact that ZnTPP forms a complex with the solvent.[32]

It should be noted that the analytical expressions for the RTPM polarization[6,30] are valid only for a relatively high diffusion coefficient,[10] which is applicable to our systems. This was confirmed by comparing the analytical results with the numerical solution of the stochastic Louiville equation.[33] Relating to our quantitative polarization results, unfortunately, quantitative polarization data of other triplet radical experiments are very scarce, and those which are available are difficult to compare with. This is because most of the systems examined are associated with a much larger ZFS parameter D.[8−10] Large D values can shorten T_1^T considerably, causing the ESPT mechanism to be negligible.

The temporal dependence of the polarization and the ability to differentiate between the ESPT and the RTPM allows the spin−lattice relaxation of the triplet (T_1^T) to be determined. Since, in most cases, direct measurement of this value in liquids such as toluene is impossible,[34] several indirect methods were employed in the past.[35,36] Our current measured values of T_1^T agree well with our previous results,[35] in which T_1^T of ZnTPP in ethanol at 243 K was calculated to be 460 ns. By adjusting this value to toluene at 250 K,[37,38] we obtain 330 ns for T_1^T, which agrees well with the present results (Table 1). Other observations[36] show much lower results for T_1^T for ZnTPP in ethanol, i.e., 28 ns, which is certainly inconsistent with our results. We cannot account directly for these discrepancies, because we have used a completely different approach to determine T_1^T. It is clear, however, that for $T_1^T \sim 30$ ns, substantial magnetization generated through ESPT in diffusion-controlled reactions is unlikely. The T_1^T values obtained for H_2-TPP are somewhat higher than ZnTPP, probably because of the much smaller ZFS parameter E of this molecule.[35,38] The values of T_1^T for H_2TPP and ZnTPP are compatible with the rotational correlation time at 230 K of ~1 ns or ~0.1 ps based upon the known BPP relation, for triplets.[35,38] The first value is more reasonable and agrees with the Debye expression for the rotational correlation time (~0.2 ns at 230 K)[38] when taking into consideration the fact that the porphyrin is planar and the Debye expression tends to be less than the actual value for this type of molecule. The results of the rotational correlation time are also in line with the results of the RTPM polarization as described above.

IV. Conclusions

An FT-EPR method for the direct measurement of the polarization generated in a triplet radical encounter is presented. This pulse method was applied to measure the polarization in Gal-H_2TPP and Gal-ZnTPP at different temperatures. In these systems, the polarization in the radical is due to two mechanisms, ESPT and RTPM, which can be differentiated, thus allowing the determination of T_1^T of the triplet molecule in liquids. The experimental results were compared to theoretical predictions and provide a good estimate of the magnitude of the exchange and distance dependence of these pairs. We believe that the present treatment may resolve some of the discrepancies found in the literature for quantitative polarization values generated by RTPM. A full theoretical model for the ESPT is currently absent, and we hope to provide a more rigorous explanation for theses differences in due course. Finally, a more descriptive name for electron spin polarization transfer (ESPT) would be triplet spin polarization transfer (TSPT).

Acknowledgment. This work is in partial fulfillment of the requirements for a Ph.D. degree (A.B.) at the Hebrew University of Jerusalem. This work was partially supported by the Israel Ministry of Science, through the "Eshkol Foundation Stipends" (A.B.), by a U.S.-Israel BSF grant, and by the Volkswagen Foundation (I/73 145). The Farkas Research Center is supported by the Bundesministerium für die Forschung und Technologie and the Minerva Gesellschaft für Forchung GmbH, FRG. We are grateful to the reviewer for his comments concerning the filling factor in the pulsed case.

References and Notes

(1) Fessenden, R. W.; Schuler, R. H. *J. Chem. Phys.* **1963**, *39*, 2147.
(2) Wong, S. K.; Wan, J. S. K. *J. Am. Chem. Soc.* **1972**, *94*, 7197.
(3) Adrian, F. J. *Rev. Chem. Intermed.* **1979**, *3*, 3.
(4) Blättler, C.; Jent, F.; Paul, H. *Chem. Phys. Lett.* **1990**, *166*, 375.
(5) Shushin, A. I. *J. Chem. Phys.* **1993**, *99*, 8723.
(6) Shushin, A. I. *Chem. Phys. Lett.* **1993**, *208*, 173.
(7) Dutt, G. B.; Periasamy, N. J. *J. Chem. Soc., Faraday Trans.* **1991**, *87*, 3815.
(8) Goudsmit, G.-H.; Paul, H.; Shushin, A. I. *J. Phys. Chem.* **1993**, *97*, 13243.
(9) Kawai, A.; Obi, K. *Res. Chem. Intermed.* **1993**, *19*, 865.
(10) Kobori, Y.; Takeda, K.; Tsuji, K.; Kawai, A.; Obi, K. *J. Phys. Chem. A* **1998**, *102*, 5160.
(11) Fujisawa, J. I.; Ohba, Y.; Yamauchi, S. *J. Phys. Chem. A* **1997**, 434.
(12) Rozenshtein, V.; Zilber, G.; Rabinovitz, M.; Levanon, H. *J. Am. Chem. Soc.* **1993**, *115*, 5193.
(13) Turro, N. J.; Koptyung, I. V.; Van Willigen, H.; McLauchlan, K. A. *J. Magn. Reson.* **1994**, *109*, 121.
(14) Imamura, T.; Onitsuka, O.; Obi, K. *J. Phys. Chem.* **1986**, *90*, 6744.
(15) Kawai, A.; Obi, K. *J. Phys. Chem.* **1992**, *96*, 52.
(16) The polarization is defined as $P = (n_\beta - n_\alpha)/(n_\beta + n_\alpha)$, where n_α and n_β are the populations in the upper and lower magnetic levels, respectively.
(17) Linear prediction was done using the MATLAB (www.mathworks.com) routine LPC, which is a general extrapolation scheme based on the principle of maximum entropy.
(18) In the experiments carried out with Gal-H_2TPP, we scattered the light over most of the sample volume with a cylindrical lens. This scattering resulted in a relatively low triplet concentration without affecting our conclusions. The laser beam was, without the lens, circular with a diameter of about 1 cm, and with the lens it was elliptical with dimensions 0.5 × 2 cm. We assume an error of ~10% in these values, due to beam inhomogeneity.
(19) Verma, N. C.; Fessenden, R. W. *J. Chem. Phys.* **1976**, *65*, 2139.
(20) The term $k_q M_y[T]$ in eq 4, neglected in pervious treatments, describes the decrease of T_2 of the radical when the triplets are generated in the solution by the laser pulse. In other words, this term contributes to the phase loss in the *XY* plane during encounter of the radical with the triplet. The ± sign in eq 5 relates to the different hyperfine lines; i.e., for each line P_m must be added or subtracted from the net polarization (P_n). In our case, P_m was found to be negligible and thus was not accounted for.
(21) Feher, G. *Bell Systems Technical J.* **1957**, 449.
(22) Blank, A.; Levanon, H. *Spectrochim. Acta A* **2000**, *56*, 363.
(23) To the best of our knowledge, the filling factor in the pulsed microwave case has not been treated yet. Since it is expected that it must be different from the conventional filling factor, defined for CW EPR experiments,[21,22] we have derived all the expressions for the pulsed cases. The present results are based on the derived expressions, which will be submitted elsewhere.
(24) Kruss, P. In *Liquids and Solutions*; Marcel Dekker: New York, 1977.
(25) Atkins, P. W. In *Physical Chemistry*, 3rd ed.; New York 1984.
(26) Wong, S. K.; Hutchinson, D. A.; Wan, J. K. S. *J. Chem. Phys.* **1973**, *58*, 985.
(27) Adrian, F. J. *J. Chem. Phys.* **1974**, *61* No. 11, 4875.
(28) The polarization was calculated with the equation[26] $P^{TM} = (4/(15\omega_z))[\omega_{ZFS}(2P_z - P_x - P_y) + 3E(P_x - P_y)]$, where ω_{ZFS} is the ZFS parameter D in rad/s, E is the noaxial term of the ZFS tensor, ω_Z is the Zeeman splitting in rad/s, and the population rates for the various triplet levels, P_x, P_y, P_z, are taken from refs 34 and 39.
(29) Salikhov, K. M.; Molin, Y. N.; Segdeev, R. Z.; Buchachenko, A. L. In *Spin polarization and magnetic effects in radical reactions*; Elsevier: Amsterdam, 1984.
(30) For weak exchange interaction, the relevant equation is $P_n = P_0$-$[1/(1 + x^2)^2 + 4/(1 + 4x^2)^2]$, where $P_0 = {}^8/_{45}[J_0 dx D^2/\lambda D_r \omega_0^2]$, $x = 1/\omega_0\tau_c$, D is the ZFS parameter, D_r is the diffusion constant, and ω_0 is the Zeeman frequency. Inserting our parameters for D, D_r, and ω_0, one cannot obtain polarization values above $\sim 0.5P_{eq}$, regardless of changes in τ_c, J_0, and λ. Moreover, the dependence of the polarization upon D_r is not consistent with our results. For strong exchange interaction, the relevant equation is $P_n = (2\pi/135)D^2/\omega_0\lambda D_r[4r_1/(4 + (\omega_0\tau_c)^2) + r_2/(1 + (\omega_0\tau_c)^2)]$, where r_1 and r_2 are the distances at which the quartet and doublet levels of the triplet radical pair cross.
(31) Adrian, F. J. *Chem. Phys. Lett.* **1994**, *229*, 465.
(32) Scherz, A.; Levanon, H. *J. Phys. Chem.* **1980**, *84*, 324.
(33) Freed, J. H.; Pedersen, J. B. *Adv. Magn. Reson.* **1976**, *8*, 1.
(34) Regev, A.; Gamliel, D.; Meiklyar, V.; Michaeli, S.; Levanon, H. *J. Phys. Chem.* **1993**, *97*, 3671.
(35) Bowman, M. K.; Toporowicz, M.; Norris, J. R.; Michalski, T. J.; Angerhofer, A.; Levanon, H. *Isr. J. Chem.* **1988**, *28*, 215.
(36) van Willigen, H.; Levstein, P. R.; Ebersole, M. H. *Chem. Rev.* **1993**, *93*, 173.
(37) Atkins, P. W.; Evans, G. T. *Mol. Phys.* **1974**, *27*, 1633.
(38) The equation for T_1 of the triplet as given ref 36 involves ZFS parameters D, E, and τ_c. $1/T_1 = D^2 j(\omega_0\tau_c) + 3E^2 j(\omega_0\tau_c)$, where $j(\omega_0\tau_c) = {}^2/_{15}\{4\tau_c/(1 + 4\omega_0^2\tau_c^2) + \tau_c/(1 + \omega_0^2\tau_c^2)\}$, where ω_0 is the Zeeman frequency. The Debye expression used for the estimation of τ_c is $\tau_c = 4\pi a^3\eta/3kT$. It is known that for spherical molecules this expression tends to overestimate τ_c.[40] However, for large planar molecules, numerical and experimental methods show that in some cases τ_c is closer and even larger than its predicted value by the simple Debye expression.[41]
(39) Regev, A.; Galili, T.; Levanon, H. *J. Chem. Phys.* **1991**, *95*, 7907.
(40) Bauer, D. R.; Brauman, J. I.; Pecora, R. *J. Am. Chem. Soc.* **1974**, *96*, 6840.
(41) Fury, M.; Jonas, J. *J. Chem. Phys.* **1976**, *65*, 2206.